Research Article | Vol. 25, No. 13 | 26 Jun 2017 | OPTICS EXPRESS 14308
Optics EXPRESS

Long period fiber grating based on periodically screw-type distortions for torsion sensing

MI DENG,[1,4] JINSHAN XU,[1,4] ZHE ZHANG,[1] ZHIYONG BAI,[1] SHEN LIU,[1] YING WANG,[1] YAN ZHANG,[1] CHANGRUI LIAO,[1] WEI JIN,[2] GANGDING PENG,[3] AND YIPING WANG[1,*]

[1]*Key Laboratory of Optoelectronic Devices and Systems of Ministry of Education and Guangdong Province, College of Optoelectronic Engineering, Shenzhen University, Shenzhen 518060, China.*
[2]*Department of Electrical Engineering, The Hong Kong Polytechnic University, Hong Kong, China*
[3]*School of Electrical Engineering and Telecommunications, University of New South Wales, Sydney 2052, NSW, Australia*
[4]*These authors contributed equally to this work*
**ypwang@szu.edu.cn*

Abstract: A novel long-period fiber grating (LPFG), fabricated by periodically cascading a series of screw-type distortions, is proposed and experimentally demonstrated. These screw-type distortions are induced by twisting the fiber during CO_2 laser beam exposure. The resulting LPFG will either be left- or right-hand helical, depending on the twist rate and direction used during fabrication, with a certain frozen shear strain. Due to the independence between grating pitch and twist rate, this type of LPFG could be more flexible than the helical- or chiral-fiber gratings reported previously. During LPFG twisting, the device displays good directional dependence and an enhanced torsion sensitivity of 0.1604 nm/(rad/m), which implies the structure could be an excellent candidate for torsion sensors.

OCIS codes: (060.2370) Fiber optics sensors; (060.2340) Fiber optics components; (050.2770) Gratings.

References and links

1. V. Lemarquand, "Synthesis study of magnetic torque sensors," IEEE Trans. Magn. **35**(6), 4503–4510 (1999).
2. L. A. Wang, C. Y. Lin, and G. W. Chern, "A torsion sensor made of a corrugated long period fibre grating," Meas. Sci. Technol. **12**(7), 793–799 (2001).
3. H. M. Kim, T. H. Kim, B. Kim, and Y. Chung, "Temperature-insensitive torsion sensor with enhanced sensitivity by use of a highly birefringent photonic crystal fiber," IEEE Photonics Technol. Lett. **22**(20), 1539–1541 (2010).
4. Z. Yan, C. Mou, K. Zhou, X. Chen, and L. Zhang, "UV-inscription, polarization-dependant loss characteristics and applications of 45° tilted fiber gratings," J. Lightwave Technol. **29**(18), 2715–2724 (2011).
5. F. Yang, Z. Fang, Z. Pan, Q. Ye, H. Cai, and R. Qu, "Orthogonal polarization mode coupling for pure twisted polarization maintaining fiber Bragg gratings," Opt. Express **20**(27), 28839–28845 (2012).
6. B. Song, H. Zhang, Y. Miao, W. Lin, J. Wu, H. Liu, D. Yan, and B. Liu, "Highly sensitive twist sensor employing Sagnac interferometer based on PM-elliptical core fibers," Opt. Express **23**(12), 15372–15379 (2015).
7. P. Zu, C. C. Chan, Y. Jin, T. Gong, Y. Zhang, L. H. Chen, and X. Dong, "A temperature-insensitive twist sensor by using low-birefringence photonic-crystal-fiber-based sagnac interferometer," IEEE Photonics Technol. Lett. **23**(13), 920–922 (2011).
8. J. Wo, M. Jiang, M. Malnou, Q. Sun, J. Zhang, P. P. Shum, and D. Liu, "Twist sensor based on axial strain insensitive distributed Bragg reflector fiber laser," Opt. Express **20**(3), 2844–2850 (2012).
9. Y. P. Wang, Y. J. Rao, Z. L. Ran, T. Zhu, and A. Z. Hu, "A novel tunable gain equalizer based on a long-period fiber grating written by high-frequency CO_2 laser pulses," IEEE Photonics Technol. Lett. **15**(2), 251–253 (2003).
10. Y. P. Wang, J. P. Chen, and Y. J. Rao, "CO_2-laser induced LPFG's torsion characteristics depending on the length of the twisted fiber," Am. J. Addict. **9**(1), 94–95 (2000).
11. Y. P. Wang and Y. J. Rao, "Long period fibre grating torsion sensor measuring twist rate and determining twist direction simultaneously," Electron. Lett. **40**(3), 164–166 (2004).
12. Y. J. Rao, T. Zhu, and Q. J. Mo, "Highly sensitive fiber-optic torsion sensor based on an ultra-long-period fiber grating," Opt. Commun. **266**(1), 187–190 (2006).

#295688 https://doi.org/10.1364/OE.25.014308
Journal © 2017 Received 10 May 2017; revised 30 May 2017; accepted 2 Jun 2017; published 13 Jun 2017

Optics EXPRESS

13. S. Oh, K. R. Lee, U. C. Paek, and Y. Chung, "Fabrication of helical long-period fiber gratings by use of a CO_2 laser," Opt. Lett. **29**(13), 1464–1466 (2004).
14. W. Shin, B. A. Yu, Y. L. Lee, Y. C. Noh, D. K. Ko, and J. Lee, "High strength coupling and low polarization-dependent long-period fiber gratings based on the helicoidal structure," Opt. Fiber Technol. **14**(4), 323–327 (2008).
15. L. Shi, T. Zhu, Y. E. Fan, K. S. Chiang, and Y. Rao, "Torsion sensing with a fiber ring laser incorporating a pair of rotary long-period fiber gratings," Opt. Commun. **284**(22), 5299–5302 (2011).
16. R. Gao, Y. Jiang, and L. Jiang, "Multi-phase-shifted helical long period fiber grating based temperature-insensitive optical twist sensor," Opt. Express **22**(13), 15697–15709 (2014).
17. L. Zhang, Y. Liu, Y. Zhao, and T. Wang, "High sensitivity twist sensor based on helical long-period grating written in two-mode fiber," IEEE Photonics Technol. Lett. **28**(15), 1629–1632 (2016).
18. L. Xian, P. Wang, and H. Li, "Power-interrogated and simultaneous measurement of temperature and torsion using paired helical long-period fiber gratings with opposite helicities," Opt. Express **22**(17), 20260–20267 (2014).
19. L. P. Sun, J. Li, L. Jin, and B. O. Guan, "Structural microfiber long-period gratings," Opt. Express **20**(16), 18079–18084 (2012).
20. G. Yin, Y. Wang, C. Liao, J. Zhou, X. Zhong, G. Wang, B. Sun, and J. He, "Long Period Fiber Gratings Inscribed by Periodically Tapering a Fiber," IEEE Photonics Technol. Lett. **26**(7), 698–701 (2014).
21. X. Y. Zhong, Y. P. Wang, C. R. Liao, G. L. Yin, J. T. Zhou, G. J. Wang, B. Sun, and J. Tang, "Long period fiber gratings inscribed with an improved two-dimensional scanning technique," IEEE Photonics J. **6**(4), 8 (2014).
22. G. M. Rego, J. L. Santos, and H. M. Salgado, "Polarization dependent loss of arc-induced long-period fibre gratings," Opt. Commun. **262**(2), 152–156 (2006).
23. M. Yang, Y. Li, and D. N. Wang, "Long-period fiber gratings fabricated by use of defocused CO_2 laser beam for polarization-dependent loss enhancement," J. Opt. Soc. Am. B **26**(6), 1203–1208 (2009).

1. Introduction

Optical fiber torsion sensors are widely used in many practical applications, such as automotive industry and anthropomorphic robots, because of their unique advantages. They are lightweight, small, flexible, compact, and most importantly, feature a high torsion sensitivity [1]. As a result, several optical in-fiber torsion sensors have been proposed using various types of fiber components, such as corrugated long-period fiber gratings (LPFGs) [2], high-birefringence fibers [3], UV inscription-tilted fiber gratings [4], polarization-maintaining fiber Bragg gratings [5], Sagnac loop structures [6, 7], and distributed Bragg reflector fiber grating lasers [8]. However, many of these proposed structures are torsion-independent and can distinguish the angle but not the direction (clockwise or counter-clockwise) of the applied torsion. As such, despite their high torsion sensitivity, they are impractical for certain applications [2, 4, 5]. CO_2 laser-induced LPFGs (C-LPFG) exhibit clear torsion dependence because of unilateral exposure to the laser beam. Various CO_2 laser inscription-based LPFG torsion sensors have been proposed, but their dynamic range is typically narrow and the torsion response often includes nonlinearity [9–12].

The potential for a new type of CO_2 laser-based LPFG with a helical structure has attracted a lot of attention since it was first proposed and demonstrated to be a good optical fiber torsion sensor [13, 14]. When torsion stress is applied, the helical pitch is effectively reduced or enhanced, resulting in good structural torsion dependence and a sensitivity that is relatively higher than conventional CO_2 laser-based LPFGs. Because of their unique benefits, helical structures have been implemented in a variety of fiber optic torsion sensors in order to achieve higher torsion sensitivities [15–19]. However, fabrication of a helical structure is very difficult, as it requires high-precision control of the twist rate, the velocity of translation stages, and the power of the laser. Additionally, the grating pitch of helical structures is dominated by a spiral freeze stress formed by rotators and the laser beam, which is inflexible because the grating pitch remains fixed once the twist rate is set.

In this letter, we report on a new fabrication method for a pre-twisted long-period fiber grating (PT-LPFG) that could be used as a torsion sensor to measure twist rate and determine rotation direction (clockwise or counterclockwise), simultaneously. The PT-LPFG was fabricated by periodically twisting a conventional single mode fiber (SMF, Coring SMF-28e +) under CO_2 laser beam irradiation to create a series of permanent screw-type fiber deformations in which the shear strain was frozen out. During fabrication, the left- or right-

Optics EXPRESS

hand helical distortion is formed in each pitch of the PT-LPFG, which is determined by the twist and horizontal translation directions. Torsional characteristics were experimentally investigated for both right- and left-hand helical PT-LPFGs and results show that the proposed sensor exhibits good torsion direction dependence and an enhanced sensitivity up to 0.1604 nm/(rad/m), which is more than five times higher than that of a conventional CO_2 laser-based long period fiber grating.

2. Fabrication system

A schematic diagram of the fabrication process for the presented PT-LPFG is shown in Fig. 1(a). It consists of an industrial CO_2 laser (SYNRAD 48-1) with a maximum power of 10 W, a three-dimensional (3D) translation stage that automatically moves together with the fiber holder (right and left horizontal directions) with a repeatable accuracy of 80 nm, and a pair of electronic rotators (Elliot Scientific MDE235) with a high rotation precision of 1". A Labivew control program with a user-friendly operation interface was developed to control every electronic device in the system such as the shutter, fiber rotators, and (3D) translation stages.

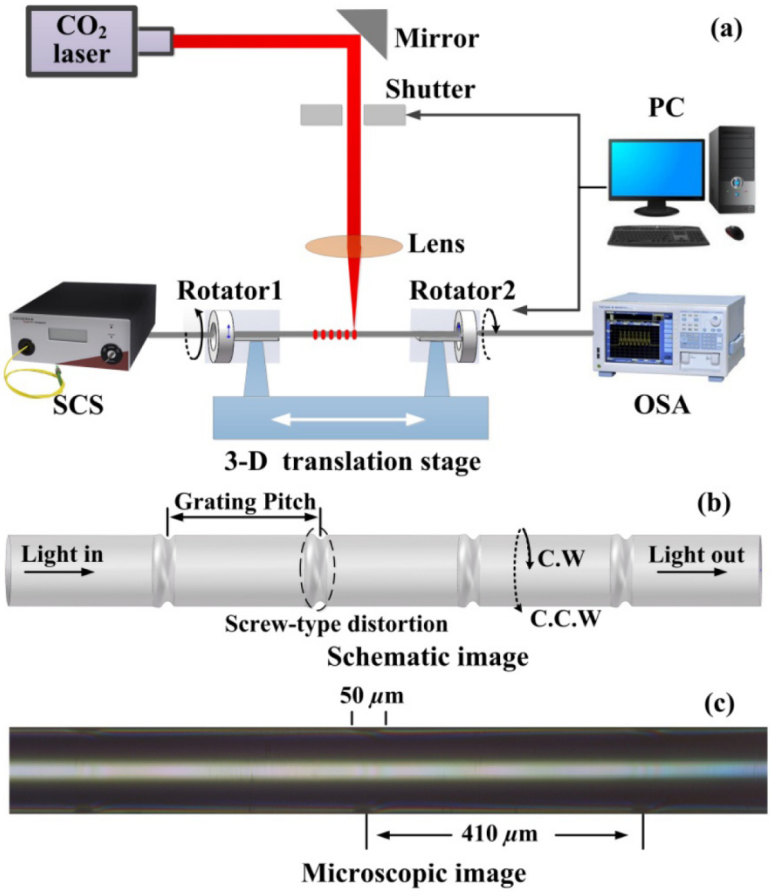

Fig. 1. (a) A sketch of the experimental setup for PT-LPFG fabrication. The (b) schematic image and (c) microscopic image of a right-hand helix PT-LPFG with fabrication parameters of Λ = 410 μm, $\beta = \pi/2$, and ν = 5°/s. The c.w and c.c.w are respectively defined as the clockwise and counter clockwise direction along the light propagating. The pre-twist rate with c.w and c.c.w direction will induce the right-and left-hand helix screw type deformation, respectively.

Optics EXPRESS

The PT-LPFG was fabricated as follows. First, the SMF was held and slightly straightened by the two fiber holders fixed on the motor rotators, ensuring the SMF core was located in the focal plane of the CO_2 laser. Second, the laser and the two rotators were activated simultaneously. The beam was then switched with a shutter and used to melt fiber in the irradiated area while the two rotators twisted the melted fiber in opposite directions. Exposure time for the CO_2 laser was dependent on the preset rotation angle β and the rotation velocity ν to ensure the shutter was closed when the rotators stopped. In this manner, a screw-type distortion fiber was easily fabricated. Finally, the 3D translation stage was moved the desired distance Λ longitudinally along the fiber. This fabrication process was then repeated several times in the same rotation angle β to produce the final PT-LPFG.

Figs. 1(b) and 1(c) show schematic and microscopic diagrams of the PT-LPFG. The screw-type areas are independent of the interval length between two neighboring regions. This implies that the preset rotation angle β, which is related to the initial twist rate τ_0, is independent of grating pitch. As a result, the final sensor includes a higher degree of design flexibility than that of a chiral fiber grating [13], which features a close correlation between twist rate and grating pitch. In addition, the fabricated PT-LPFG and chiral fiber grating can either be left- or right-helix, as determined by the twist and horizontal translation directions.

3. Spectra characteristics

The transmission spectrum of the PT-LPFG was measured by a super-continuum light source (SCS, NKT Photonics Super K Compact) and an optical spectrum analyzer (OSA, YOKO-GAWA AQ6370C). We fabricated the PT-LPFG with a grating pitch of 410 μm and $\beta = \pi/3$. The measured transmission spectra, which featured an increasing number of periods, was recorded and is plotted in Fig. 2. The resonant intensity was enhanced by the increased periodicity and achieved a maximum of −32.5 dB at a wavelength of 1552.4 nm when 24 periods were included. Using an infrared camera, we observed the near field intensity profile for the PT-LPFG. As shown in the inset image in Fig. 2, a clear asymmetrical cladding mode field LP16 profile was obtained at the resonant wavelength of 1552.4 nm, which is similar to that of C-LPFG [20, 21].

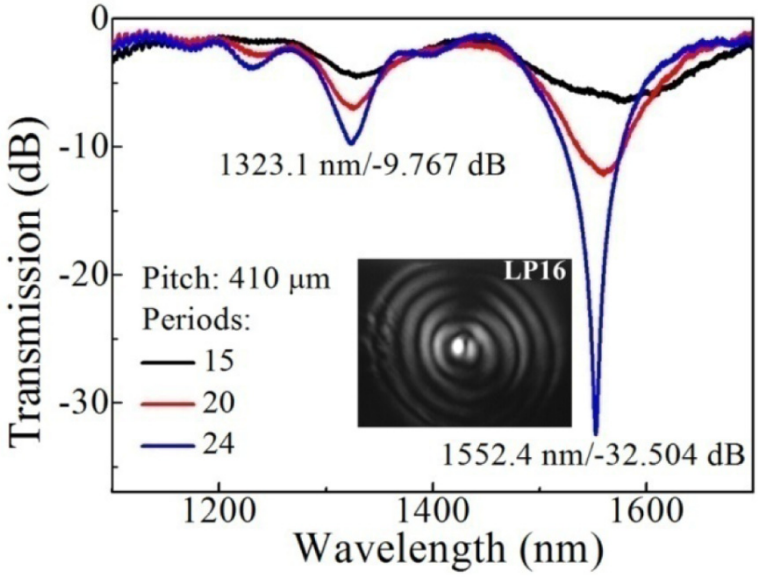

Fig. 2. The transmission spectrum evolution of a right-helix PT-LPFG with a grating pitch of 410 μm and a mode field diagram at a wavelength of 1552.4 nm

Optics EXPRESS

The physical mechanism for mode coupling in the PT-LPFG may be combined by residual stress release, changes in fiber geometry, and frozen shear stress, which can be induced in the screw-type structure. In this fabrication system, the separation L_0 between the two rotators was 0.055 m, and thus, the frozen shear strain could be quantified by the initial twist rate of $\tau_0 = 2\beta / L_0 = 2\beta / 0.055 \approx 36\beta$ (rad/m). In contrast to C-LPFGs, the proposed PT-LPFG with frozen shear strain can alter sensing and transmission characteristics.

To verify reproducibility and design flexibility, several PT-LPFGs were fabricated in two groups. The first exhibited different values of Λ and constant β, while the second included different values of β but constant Λ. In the first group, five right-helix PT-LPFGs with grating pitches of 400, 410, 420, 430, and 440 μm were manufactured with $\beta = \pi/3$. According to the phase matching conditions of typical LPFGs, the resonant wavelength shift with a change in grating pitch could be considered experimentally under a constant pre-frozen torsion stress. The corresponding resonant wavelengths were fitted and are plotted in Fig. 3. The resonant wavelength is red-shifted with the increased pitch, which coincides with that of a C-LPFG with modes coupling between core mode and lower order cladding modes.

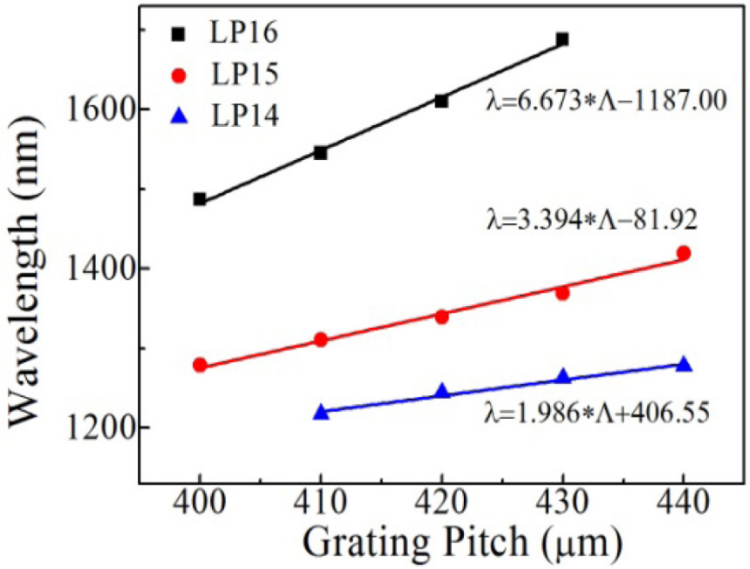

Fig. 3. Measured resonant wavelengths versus grating pitch for right-helix PT-LPFGs with the same fabrication parameters and different grating pitches of 400, 410, 420, 430, and 440 μm, with $\beta = \pi/3$ and $\Lambda = 30$.

In the second group, several left- and right-hand helix PT-LPFGs were fabricated with the same grating pitch Λ = 410 μm but with β varying from $\pi/3$ to π at intervals of $\pi/6$, corresponding to the spectra shown in Figs. 4 (a) and 4(b), respectively. As seen in the figure, with increasing β, the resonant wavelengths of the transmission spectra present a blue shift in the range from $\pi/2$ to π, which provides a new value for β to tailor the transmission spectra for practical applications.

Optics EXPRESS

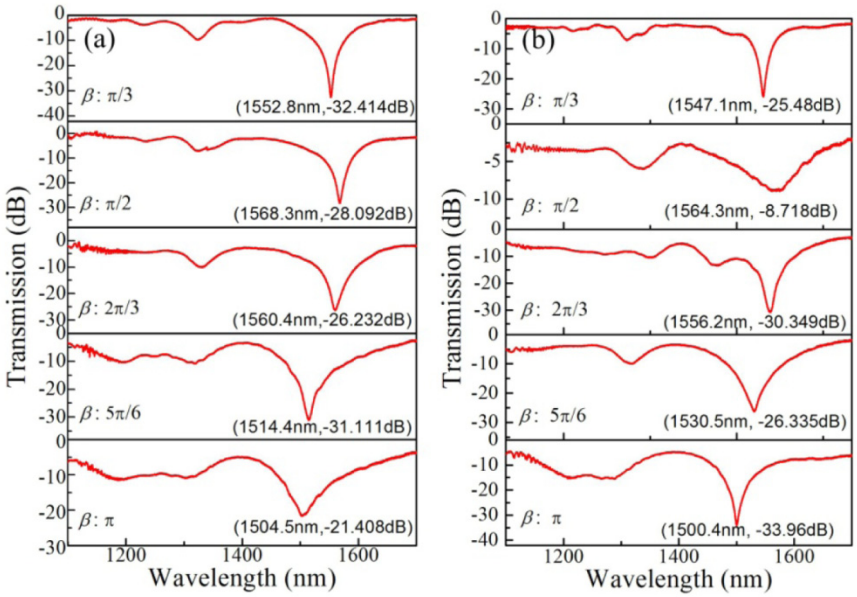

Fig. 4. The spectra of a (a) left-hand helix and (b) right-hand helix PT-LPFG with the same grating pitch $\Lambda = 410\ \mu$m but with β varying from $\pi/3$ to π in intervals of $\pi/6$.

4. Torsion characteristics

PT-LPFGs with opposite helix and C-LPFGs were fabricated for investigating torsion characteristics, the resulting transmission spectra are shown in Fig. 5. The grating pitch Λ and grating period N for each sample were 420 μm and 30, respectively. The pre-twist angle and rotation velocity for PT-LPFGs were $\beta = \pi/3$ and $\nu = 5°/s$, respectively.

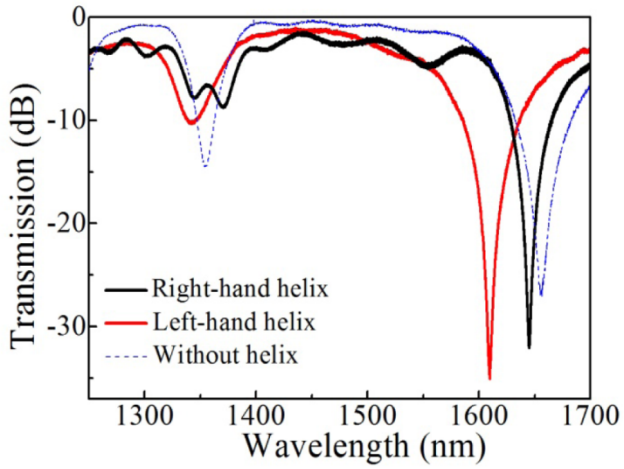

Fig. 5. The transmission spectra of two PT-LPFGs with opposite helicity and a C-LPFG without helicity under the same grating pitch of 420 μm.

We used the torsion test system shown in Fig. 6 in which two fiber holders held the LPFGs fixed. One of them could rotate clockwise or counter-clockwise, with a separation L of 55 mm. The two ends of the fiber were connected by an SCS and OSA, respectively, to measure and record the transmission spectra. The applied torsion τ was measured by the applied angle α and the twist length L, such that $\tau = \alpha / L = \alpha / 0.055 \approx 18\alpha$ (rad/m). Figures

Optics EXPRESS

7(a) and 7(b) show wavelength shifts in the transmission spectra as the applied twist rate τ varied from −57.1 rad/m to 57.1 rad/m. It is evident that with the same rotation applied, the resonant wavelength for PT-LPFGs with opposite helicity give the opposite response. When the applied torsion is clockwise, the right-helix PT-LPFG features a blue shift and the left-helix PT-LPFG a red shift. Changes in the applied torsion direction cause the right-/left-helix PT-LPFG to produce the opposite shift. Considering the relationship between grating helix and applied torsion rotation, we can conclude that co-directional torsion causes the resonance peak to shift to shorter wavelengths. The peaks shift to longer wavelengths under contra-directional torsion, similar to helicoidal LPFGs [14]. For the purpose of comparison, we fabricated a C-LPFG using the same system and measured the transmission spectra under the same torsion range; the results are presented in Fig. 7(c). This C-LPFG was fabricated without an induced helix, allowing us to take the torsional characteristics of the PT-LPFG into full consideration.

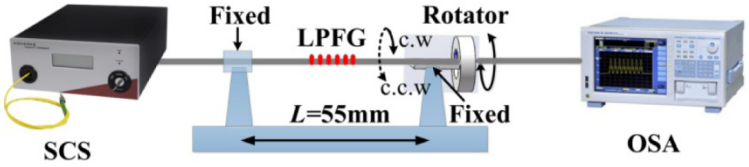

Fig. 6. A sketch of the torsion test system used for LPFGs.

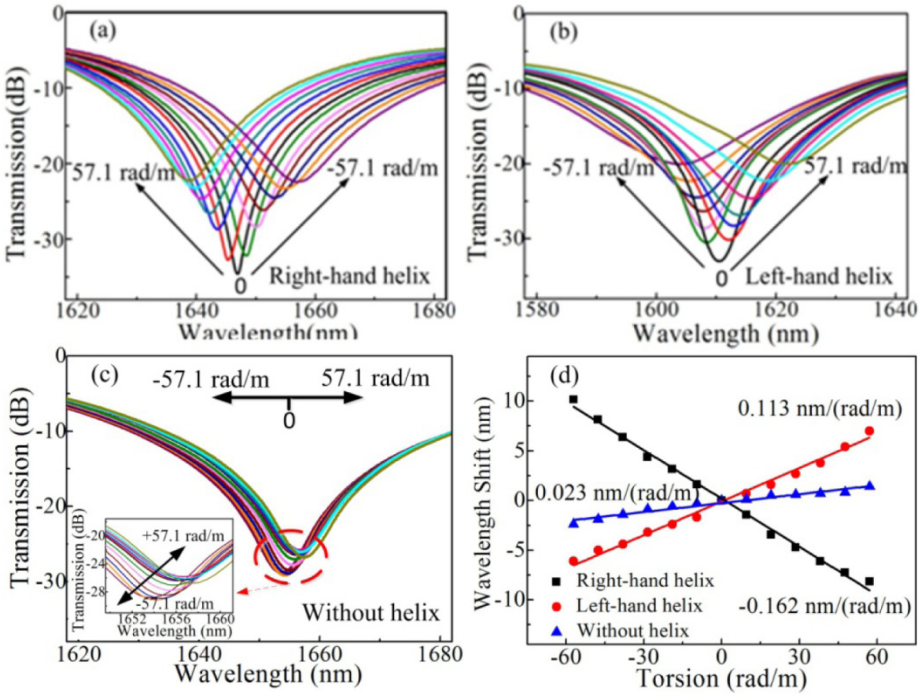

Fig. 7. Resonant wavelength shifts for (a) a right-hand helix PT-LPFG and (b) a left-hand helix PT-LPFG under an applied torsion ranging from −57.1 rad/m to 57.1 rad/m. (c) A C -LPFG without helicity with 30 grating periods and a grating pitch of 420 μm. (d) The linear fitter between the torsion and wavelength shifts for all three LPFGs.

Wavelength shifts for the three samples are plotted in Fig. 7(d). An approximately linear relationship was observed between the wavelength shift and the applied torsion during clockwise and counterclockwise rotations. As such, the data were subjected to linear fitting. Slopes indicative of the torsion sensitivities of the three PT-LPFG samples are shown in Fig.

Optics EXPRESS

7(d). This demonstrates that the frozen shear strain can effectively enhance torsion sensitivity up to 0.162 nm/(rad/m) and 0.113 nm/(rad/m) for right-/left-helix PT-LPFGs, respectively. This is over 5 times higher than conventional LPFGs, which average at ~0.023 nm/(rad/m). Also, according to the above analysis, under co-directional torsion (the effective rotation is clockwise for conventional LPFGs) the resonant wavelengths between PT-LPFG and C-LPFG provide opposite responses. This implies the frozen shear strain has affected the in-fiber polarization and altered the in-fiber modulation. In the process of testing, we twist the fiber back and forth under this range several times. A consistent repeatable change was observed in the resonant wavelengths.

5. PDL characteristic

Polarization-dependent loss (PDL) characteristics were also investigated using a PDL measurement system that consisted of a tunable laser, a photonic all-parameter analyzer, a polarization controller, and an optical power meter. Since PDL is related to the depth of the attenuation dip, we fabricated a right-helix PT-LPFG with $\beta = \pi/2$ and, for comparison, a C-LPFG with the same grating pitch of 410 μm and grating periods of 30. Both LPFGs were created with similar extinction ratios. As shown in Figs. 8(a) and 8(b), the average loss and the maximum PDL of the C-LPFG and PT-LPFG were obtained around resonant wavelengths of 1573.2 nm and 1568.6 nm, respectively. The latter exhibits a maximum PDL of 3.6 dB, which is relatively smaller than that of the former (5.4 dB) and previously reported values [22, 23]. Because of the pre-twisting procedure, the asymmetrical RI modulation caused by the CO_2 laser was reduced, causing the PT-LPFG PDL to be smaller than that of the C-LPFG. Pre-twisting the fiber can freeze out in-fiber stress causing the structure to attach the same RI modulation with lower energy, as compared with a conventional LPFG fabricated by scanning up and down. Lower energies are needed to fabricate a PT-LPFG that may have caused the PDL to be smaller.

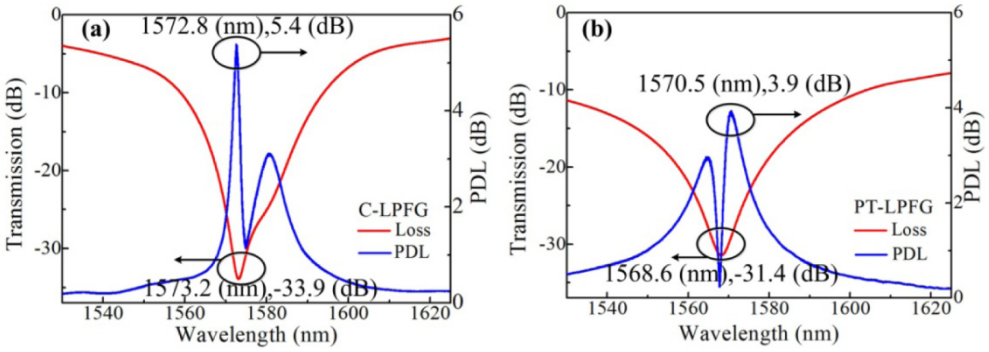

Fig. 8. The PDL of a (a) C-LPFG and (b) a right-hand helix PT-LPFG for $\beta = \pi/2$ with the same grating pitch of Λ = 410 μm and 30 grating periods (N).

6. Conclusion

In summary, we have proposed a novel PT-LPFG. Experimental results verified the design has several practical benefits. First, the proposed PT-LPFGs have significant design flexibility due to the independence of grating modulation area and grating pitch. Second, both of the left- and right-handed PT-LPFGs could distinguish torsion direction and measure twist rate with an enhanced sensitivity. Moreover, the proposed PT-LPFGs have relatively lower polarization dependence loss, which is ideal for optical communication.

Optics EXPRESS

Acknowledgments

This work was supported by National Natural Science Foundation of China (grant nos. 61425007, 61377090, and 61575128), Guangdong Provincial Department of Science and Technology (grants nos. 2014A030308007, 2014B050504010, 2015B010105007 and 2015A030313541), Science and Technology Innovation Commission of Shenzhen (grants nos. ZDSYS20140430164957664, GJHZ20150313093755757, KQCX20140512172532195, JCYJ20150324141711576), China Postdoctoral Science Foundation (2015M582404, 2015M582406) and Pearl River Scholar Fellowships.